J. Membrane Biol. 88, 187–198 (1985)

The Journal of
Membrane Biology
© Springer-Verlag 1985

Conformational States of Sarcoplasmic Reticulum Ca^{2+}-ATPase as Studied by Proteolytic Cleavage

Jens P. Andersen and Peter L. Jørgensen
Institute of Physiology, University of Aarhus, 8000 Aarhus C, Denmark

Summary. Conformational states in sarcoplasmic reticulum Ca^{2+}-ATPase have been examined by tryptic and chymotryptic cleavage. High affinity Ca^{2+} binding (E_1 state) exposes a peptide bond in the A fragment of the polypeptide chain to trypsin. Absence of Ca^{2+} (E_2 state) exposes bonds in the B fragment, which are protected by binding of Mg^{2+} or ATP. After phosphorylation from ATP the tryptic cleavage pattern depends on the predominant phosphoenzyme species present. ADP-sensitive E_1P and ADP-insensitive E_2P have cleavage patterns identical to those of unphosphorylated E_1 and E_2, respectively, indicating that two major conformational states are involved in Ca^{2+} translocation. The transition from E_1P to E_2P is inhibited by secondary tryptic splits in the A fragment, suggesting that parts of this fragment are of particular importance for the energy transduction process.

The tryptic cleavage patterns of phosphorylated forms of detergent solubilized monomeric Ca^{2+}-ATPase were similar to those of the membrane-bound enzyme, indicating that Ca^{2+} translocation depends mainly on structural changes within a single peptide chain. On the other hand, the protection of the second cleavage site as observed after vanadate binding to membranous Ca^{2+}-ATPase could not be achieved in the soluble monomeric enzyme. Shielding of this peptide bond may therefore be due to protein-protein interactions in the semicrystalline state of the vanadate-bound Ca^{2+}-ATPase in membranous form.

Key Words protein structure · trypsin · chymotrypsin · Ca^{2+} transport · phosphorylation · energy transduction · detergent

Introduction

The molecular mechanism of Ca^{2+} transport by sarcoplasmic reticulum Ca^{2+}-ATPase provides an intriguing problem [42]. This enzyme can be prepared in pure form in a membrane-bound as well as a soluble state [32]. Although Ca^{2+}-ATPase may form oligomeric complexes in the membrane [2, 19, 43], there is now good evidence that the minimal functional unit in energy coupling is a single 115-kD peptide [3, 4, 29]. A phosphorylated form of the Ca^{2+}-ATPase peptide provides the link between ATP hydrolysis and Ca^{2+} translocation. Based on chemical quench studies of phosphorylation and dephosphorylation reactions the minimal transport cycle

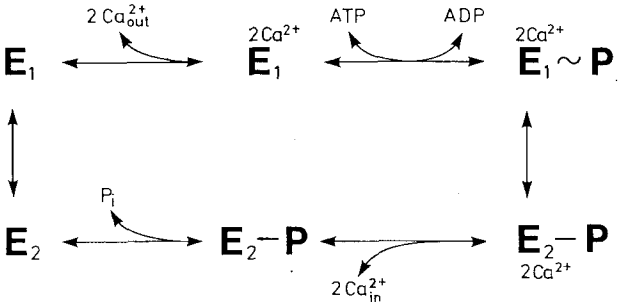

shown as Scheme 1 has been proposed [10]. In this cycle, translocation of Ca^{2+} is accomplished by alteration between two major conformations, E_1 and E_2, with different affinity and orientation of their Ca^{2+} binding sites. Energy transfer between the phosphorylation site and the Ca^{2+} sites occurs in relation to the E_1P to E_2P transition. The existence of two states of both dephosphoforms and phosphoforms of the protein has been deduced from studies of ligand binding and intermediary reactions. Evidence for two structurally distinct conformations of dephosphoforms of the protein has been obtained by experiments monitoring Ca^{2+}-induced fluorescence changes [4, 11, 18, 35], changes in mobility of covalently attached spinlabels [7, 9] and by titrations of the accessibility of side-chain groups of the Ca^{2+}-ATPase protein [34, 46].

Structural evidence for the existence of two distinct phosphoprotein conformations is less convincing. Changes in intensity of intrinsic tryptophan fluorescence accompanying transition from ADP-sensitive (E_1P) to ADP-insensitive (E_2P) phosphoenzyme are smaller than those associated with E_1-E_2 transitions of the unphosphorylated protein [3]. Although the change in the chemical reactivity of the phosphorylated aspartic acid residue towards ADP during the enzymatic cycle is closely linked to a decrease in affinity of the two Ca^{2+} transport sites [3], these events are not necessarily associated with

Fig. 1. Tryptic cleavage of sarcoplasmic reticulum protein. Sarcoplasmic reticulum vesicles were digested with trypsin (1 μg/100 μg protein) for 30 min at 20°C in 50 mM Tes/Tris (pH 7.5), 0.3 M sucrose. Other additions are described below. *A* is a control (0.1 mM $CaCl_2$ present) in which buffer was added instead of trypsin. In *B* and *C* 0.1 mM $CaCl_2$ or 1 mM EGTA were present, respectively. In *D* the vesicles were preincubated 1 hr in the presence of 1 mM EGTA, 1 mM $MgCl_2$ and 500 μM Na_3VO_4 before addition of trypsin. The samples were centrifuged and processed for gel electrophoresis as described in Materials and Methods

changes in protein structure [37]. Other features such as "occlusion" of Ca^{2+} in E_1P [12, 41] and increased hydrophobicity in the catalytic site in E_2P [10, 14] point to presumptive structural differences between the two phosphoforms. Hybrid conformations between the major states outlined in Scheme 1 has been suggested by fluorescence changes associated with binding of Mg^{2+} and ATP in the absence of Ca^{2+} [8, 13].

The techniques referred to above have not allowed localization of structural changes within the protein, and the magnitude of the conformational change in terms of the number of residues involved in motion within the protein remains uncertain. More direct probes of protein structure are also required to discern local effects of ligand binding from the major conformational changes associated with cation translocation. Another question of basic importance is whether interaction between subunits of Ca^{2+}-ATPase with M_r 115,000 is required for conformational changes related to active cation transport or if the conformational change can occur within a protomer peptide chain.

The goal of the present study has been to examine the major conformational states of Ca^{2+}-ATPase by use of graded proteolytic digestion. Previous studies showed that rather detailed structural information about the two conformations of Na^+,K^+-ATPase could be obtained with the aid of proteolytic enzymes [23]. In the protein of Ca^{2+}-ATPase the proteolytic splits have been considered to be indifferent points in the primary sequence, but recently different tryptic cleavage patterns of E_1 and E_2 forms of Ca^{2+}-ATPase have been suggested [21, 28]. We have examined the time courses of tryptic inactivation of Ca^{2+}-ATPase activity and cleavage of the protein with and without Ca^{2+} and other ligands to test their effect on the digestion patterns, both in phosphorylating and nonphosphorylating conditions. Our data indicate that the two phosphorylated intermediates, E_1P and E_2P, are associated with different protein structures, which with respect to the tryptic cleavage patterns resemble the unphosphorylated E_1 and E_2 conformations, thus supporting the notation in Scheme 1. Similar cleavage patterns were demonstrated for membrane-bound and soluble monomeric Ca^{2+}-ATPase, indicating that the E_1-E_2 conformational transition does not require subunit interaction.

Materials and Methods

Sarcoplasmic reticulum vesicles and purified Ca^{2+}-ATPase in membranous form were prepared as previously [4]. For proteolytic digestion membranes (usually 0.5 mg protein/ml) were incubated at 20°C with 1 or 5 μg TPCK-trypsin[1] (Merck) per 100 μg protein in buffer media containing 50 mM Tes/Tris (pH 7.5 or 8.0) with various additions of sucrose, NaCl, $CaCl_2$, $MgCl_2$, EGTA, ATP, Na_3VO_4 and the non-ionic detergent $C_{12}E_8$ as described in the figure legends. The digestion was terminated by addition of soybean trypsin inhibitor (4 μg/μg trypsin) and subsequent cooling at 0°C. Chymotryptic cleavage of the Ca^{2+}-ATPase was performed in similar conditions. This reaction was terminated by supplementing with salt to a high concentration, 300 mM, NaCl, and cooling to 0°C.

The digested samples were used directly for gel-electrophoretic analysis of the peptides and measurement of Ca^{2+}-transport, Ca^{2+}-ATPase activity and phosphorylation. In a few experiments trypsin together with trypsin inhibitor were removed before electrophoresis by sedimentation of the membranes by centrifugation.

Digestion of nitrated casein (Calbiochem) with trypsin was performed in the same conditions as for tryptic digestion of Ca^{2+}-ATPase (at pH 8.0). The proteolytic activity was determined after precipitation of undegraded protein with trichloroacetic acid followed by centrifugation as previously described [24].

[1] *Abbreviations:* $C_{12}E_8$, octaethyleneglycol monododecyl ether; Tes, N-(tris-[hydroxymethyl] methyl-2-amino) ethanesulfonic acid; EGTA, ethyleneglycol bis (β-aminoethyl ether) - N,N,N',N'-tetraacetic acid; TPCK, tosylamide-phenylethyl-chloromethyl-ketone. AdoPP[NH]P, adenosine 5'-[β,γ-imido] triphosphate.

Ca^{2+}-ATPase activity was measured at 20°C by a NADH-coupled assay [33] in the presence of 10 mM Tes (pH 7.5), 0.1 M KCl, 0.1 mM $CaCl_2$, 1 mM $MgCl_2$ and 5 mM MgATP with or without the presence of 0.5 mg/ml $C_{12}E_8$. ATP-driven Ca^{2+}-uptake into sarcoplasmic reticulum vesicles during 5 min incubation with $^{45}Ca^{2+}$ in phosphate buffer was measured after gel filtration on small Sephadex columns as previously [5].

Phosphorylation of Ca^{2+}-ATPase peptides with [γ^{32}P]-ATP was carried out at 0°C for 30 sec as previously described [3] in 50 mM Tes/Tris buffer (pH 8.0), 30 mM NaCl, 25 μM [γ^{32}P]-ATP at 1 or 200 μM free Ca^{2+} and 10 mM Mg^{2+}. In some experiments dephosphorylation in the presence of 1 mM ADP + 1 mM EGTA was allowed to occur for 5 sec before acid quenching. The acid denatured protein was washed and radioactivity and protein were determined as before [3]. Samples for electrophoresis were washed only once.

For gel-electrophoretic analysis of tryptic and chymotryptic peptides from Ca^{2+}-ATPase the protein samples were mixed with $NaDodSO_4$ and mercaptoethanol (final concentrations 2 and 1%, respectively) and incubated for 3 min at 100°C. The aliquots were subjected to $NaDodSO_4$ polyacrylamide gel electrophoresis in 5–15% gradient slab gels prepared according to Laemmli [25] with omission of the stacking gel. The gels were stained and destained in 40% methanol and 10% acetic acid with and without 0.25% Coomassie Brilliant Blue R-250, respectively. Quantitative gel scanning was preformed with a LKB 2202 Ultroscan Laser Densitometer. Apparent molecular weights were estimated by assuming a linear relationship between the logarithm of molecular weight and log T% [38] using pyruvate kinase (M_r = 57,000), lactate dehydrogenase (M_r = 33,000) and trypsin inhibitor (M_r = 21,000) for standardization.

Polyacrylamide gels (5–15%) used for electrophoresis of phosphorylated peptides in $NaDodSO_4$ at pH 2.4 were prepared by the general procedure described by Avruch and Fairbanks [6]. Gradient slab gels (5–15 T%, 3.6 C%) were formed in 1% $NaDodSO_4$, 50 mM Na-phosphate, pH 2.4, using 1 mg/ml ascorbic acid, 2.5 μg/ml $FeSO_4$ and 0.003% H_2O_2 for catalysis of crosslinking. The washed acid denatured phosphoprotein (100–200 μg) was dissolved in 80 μg 2% $NaDodSO_4$/10 mM dithiothreitol/50 mM Na-phosphate, pH 2.4. One drop of 40% glycerol and 5 μl of 360 μg/ml pyronin Y were added, and the phosphorylated peptides were separated by electrophoresis for 3–4 hr (4–5 mA per gel) at pH 2.4, 15°C. After 7–9 cm migration of the pyronin dye front, the lanes were cut out and sliced (3 mm) and counted by Cerenkov irradiation. The recovery of phosphorylation was 3.2–3.5 nmol/mg protein in undigested samples, representing approx. 80% of the phosphorylation of controls not subjected to electrophoresis.

Calculation of *p*Ca values was based on published stability constants for complexation of Ca^{2+} and Mg^{2+} with EGTA [45].

Results

Figure 1 shows gel patterns of sarcoplasmic reticulum vesicles digested with trypsin (1 μg/100 μg sarcoplasmic reticulum protein) for 30 min with and without free Ca^{2+} present, and after binding of vanadate in absence of Ca^{2+}. Trypsinolysis is known to produce two primary fragments (A and B) of apparent molecular mass 50–60 and 45–55 kD, respectively [20, 22, 31, 40, 44]. According to these original studies, secondary fragments with apparent molecular weight 30,000–33,000 (A_1) and 20,000–24,000 (A_2) are formed on prolonged incubation of Ca^{2+}-ATPase with trypsin. In the present work secondary splitting was also observed, both with and without free Ca^{2+} (Fig. 1*B* and *C*), but not after binding of vanadate (Fig. 1*D*) in accordance with results obtained by Dux and Martonosi [15]. In absence of vanadate at least three subspecies of A_1 could be identified. Two closely migrating bands, which we group together as A_1' and a third band which is well separated from the others and is designated A_1''. Calibration with standard proteins shows that A_1' and A_1'' peptides have apparent molecular weights approximately 37,000 and 33,000, respectively. A_1'' appears later than A_1' and may be a cleavage product of A_1'. The relative concentrations of the secondary fragments depend on the presence of micromolar-free Ca^{2+}. With Ca^{2+} the concentration of A_1'' fragment is higher than in the absence of Ca^{2+}. Peptides migrating between B and A_1' (designated X_1 and X_2), which most likely are derived from the B fragment (*see* below), are observed only after digestion in absence of free Ca^{2+}. It is also seen that the extrinsic protein, calsequestrin (a usual component of sarcoplasmic reticulum vesicles) is degraded by trypsin in the absence of Ca^{2+} and vanadate, but not in the presence of either one of these ions. This indicates that the membrane is destabilized by digestion in absence of Ca^{2+}-ATPase ligands since calsequestrin is located at the interior surface of the sarcoplasmic reticulum vesicle [30, 40]. In accordance with this interpretation we found that ATP-driven net uptake of Ca^{2+} into the vesicles disappears after tryptic digestion in absence of Ca^{2+}, whereas Ca^{2+}-ATPase activity is stimulated (Table 1). After trypsinolysis in presence of Ca^{2+}, Ca^{2+}-uptake and Ca^{2+}-ATPase activity declined in parallel (Table 1). Thus there was no evidence for a

Table 1. Effect of tryptic cleavage on Ca^{2+} uptake and Ca^{2+}-ATPase activity in sarcoplasmic reticulum vesicles

Conditions of tryptic digestion	Remaining activity after 30 min digestion		
	Ca^{2+}-ATPase		Ca^{2+} uptake (%)
	Vesicle (%)	Soluble (%)	
− Ca^{2+} (+EGTA)	171	80	6.4
+ Ca^{2+}	67	68	65

Ca^{2+} uptake and Ca^{2+}-ATPase activity were measured immediately after termination of digestion as described in Materials and Methods. Values for samples corresponding to Fig. 1*B* and *C* are shown as percentage of controls incubated likewise, but in absence of trypsin. Soluble Ca^{2+}-ATPase refers to the unmasked Ca^{2+}-ATPase activity measured in presence of $C_{12}E_8$.

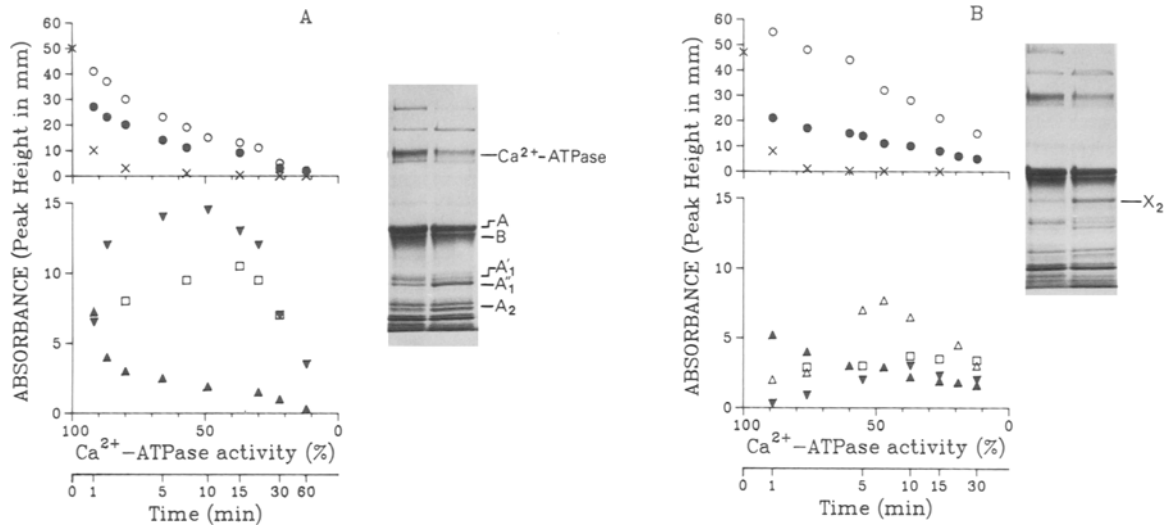

Fig. 2. Relation between tryptic digestion and inactivation of Ca^{2+}-ATPase activity in presence and absence of Ca^{2+}. Purified Ca^{2+}-ATPase membranes were incubated with trypsin (5 μg/100 μg Ca^{2+}-ATPase) at 20°C for various times as described in Materials and Methods in presence of 30 mM NaCl, 50 mM Tes/Tris (pH 8.0) and either 50 μM $CaCl_2$ (*A*) or 1 mM EGTA (*B*). Ca^{2+}-ATPase activity was measured immediately after termination of digestion, and the samples were subjected to gel electrophoresis without prior washing. Relative protein concentration of the various tryptic fragments (peak heights of the elecrophoretograms obtained by quantitative gel scanning) is shown as a function of remaining Ca^{2+}-ATPase activity or time of trypsinolysis. X, 115,000 kD Ca^{2+}-ATPase chain; ○, A fragment; ●, B fragment; △, X_2 fragment; ▲, A_1' fragment; ▼, A_1'' fragment; □, A_2 fragment. The photographs show gels corresponding to 1 and 5 min digestion

"true" uncoupling of Ca^{2+} translocation from ATP hydrolysis induced by the tryptic splits shown in Fig. 1.

Figure 2 provides a detailed account of the relationship between Ca^{2+}-ATPase activity (V_{max}) of purified (leaky) Ca^{2+}-ATPase vesicles and the concentrations of the major fragments estimated by gel scanning after various durations of incubation with trypsin (5 μg/100 μg Ca^{2+}-ATPase) in presence and absence of Ca^{2+} at pH 8.0, 30 mM NaCl. The latter conditions were chosen to be able to obtain well-defined phosphorylated states of the protein in presence of ATP (*cf.* Fig. 6) as well as a relatively fast rate of proteolysis. As can be seen in Fig. 2 the cleavage patterns are basically similar to those observed for sarcoplasmic reticulum vesicles. A characteristic feature is that with Ca^{2+}, A_1'' is present in larger quantities than without Ca^{2+}. The A and A_1' fragments disappear faster when Ca^{2+} is present than in its absence, suggesting that the high concentration of A_1'' in presence of Ca^{2+} results from an increased rate of formation under these conditions rather than a decreased rate of further degradation. With Ca^{2+}, formation of A_2 is seen to occur faster than without Ca^{2+}. The nonlinear dependence of A on Ca^{2+}-ATPase activity in Fig. 2*A* suggests that the catalytic function is at least partially preserved after secondary cleavage in the A fragment. In absence of Ca^{2+} (Fig. 2*B*) the concentration of secondary fragments derived from A is relatively low, and the dependence of Ca^{2+}-ATPase activity on the presence of A fragment is almost linear. The X_1 and X_2 fragments could be observed also for the purified Ca^{2+}-ATPase preparation after tryptic cleavage in absence of Ca^{2+} (and Mg^{2+}, *see below*). However, for unknown reasons the concentration of X_1 fragment was variable and quite low in some experiments. Therefore only the X_2 fragment (apparent molecular mass approximately 45 kD) can be considered to be a characteristic feature of the tryptic cleavage pattern observed in absence of Ca^{2+} (*cf.* Fig. 2*B*).

Chymotrypsin cleaves Ca^{2+}-ATPase in patterns that are different from those observed with trypsin. It is seen from Fig. 3 that an 80-kD fragment is formed as a result of primary chymotryptic cleavage. Another chymotryptic split gives rise to fragments of molecular mass 50–55 kD. Secondary cleavage of these fragments is accelerated when Ca^{2+} is bound with high affinity to the pump protein. Particularly two fragments (arrow, Fig. 3) of apparent molecular weight close to 30,000 are more prominent after chymotryptic cleavage in the presence of micromolar concentrations of Ca^{2+} than in its absence. The effect of Ca^{2+} on chymotryptic cleavage patterns thus bears some resemblance to the Ca^{2+} induced change in tryptic digestion pattern. However, the Ca^{2+} effect is more distinct with

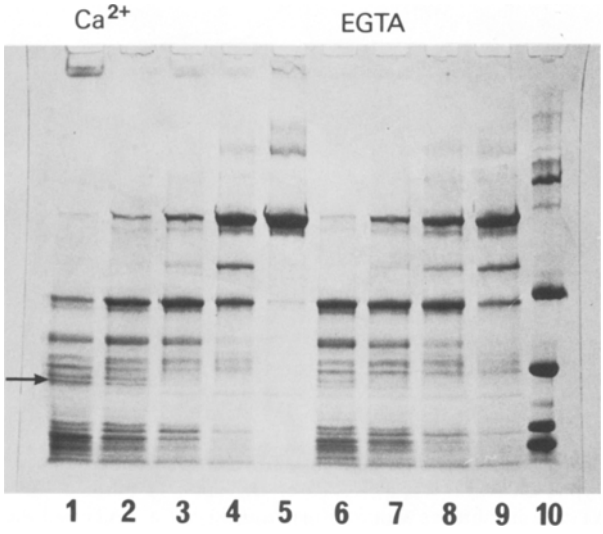

Fig. 3. Chymotryptic digestion of purified Ca^{2+}-ATPase membranes in presence and absence of Ca^{2+}. Ca^{2+}-ATPase (0.5 mg/ml) was treated with various concentrations of chymotrypsin for 5 min at 20°C in 15 mM Tes/Tris buffer, pH 8.0, 10 mM NaCl with either 50 μM $CaCl_2$ (lanes 1–5) or 1 mM EGTA (lanes 6–9). The chymotrypsin concentrations corresponding to lanes 1–9 (from left to right) were: 25 μg/ml; 10 μg/ml; 4 μg/ml; 1 μg/ml; 0 μg/ml; 25 μg/ml; 10 μg/ml; 4 μg/ml; 1 μg/ml. The calibration mixture in lane 10 consisted of pyruvate kinase (M_r = 57,000), lactate dehydrogenase (M_r = 33,000), trypsin inhibitor (M_r = 21,000) and cytochrome *c* (M_r = 12,000)

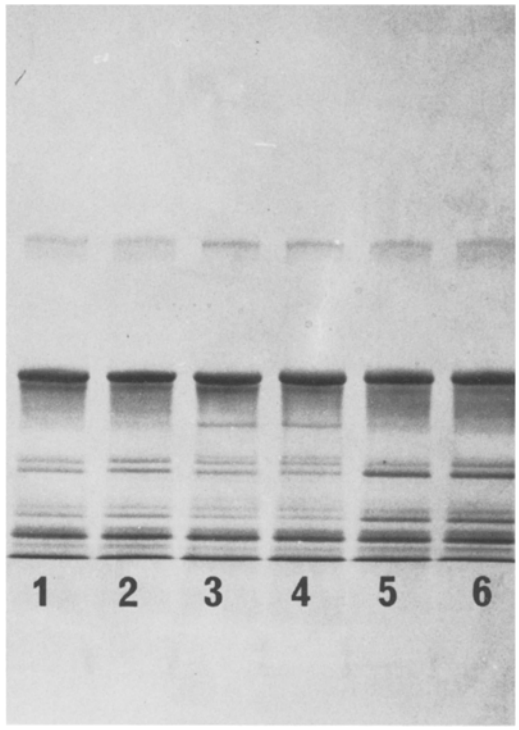

Fig. 4. Effect of Mg^{2+} on tryptic cleavage of Ca^{2+}-ATPase in presence and absence of Ca^{2+}. Digestion of purified Ca^{2+}-ATPase membranes with trypsin (5 μg/100 μg Ca^{2+}-ATPase) was performed for 5 min at 20°C in 30 mM NaCl, 50 mM Tes/Tris (pH 8.0) as described in Materials and Methods. 1 mM EGTA was present in all samples and $CaCl_2$ and $MgCl_2$ were added to produce the concentrations of free ions indicated below. Lane 1: $<10^{-9}$ M Ca^{2+}, 2 mM Mg^{2+}. Lane 2: $<10^{-9}$ M Ca^{2+}, 10 mM Mg^{2+}. Lane 3: $<10^{-9}$ M Ca^{2+}. Lane 5: 10^{-7} M Ca^{2+}. Lane 6: 10^{-7} M Ca^{2+}, 10 mM Mg^{2+}. The sample in lane 4 was similar to that in lane 3 except for the presence of 60 mM NaCl

trypsin, and we therefore use this enzyme for further studies of ligand effects on the structure of Ca^{2+}-ATPase.

Figure 4 shows effects of Mg^{2+} concentration on the tryptic cleavage pattern after 5 min digestion in presence and absence of Ca^{2+}. Addition of Mg^{2+}, in presence of Ca^{2+} (lane 6), does not change the digestion pattern significantly. In absence of Ca^{2+}, addition of Mg^{2+} (2 or 10 mM) causes disappearance of the X_2 fragment, but the characteristic distribution of A'_1 and A''_1 peptides is only slightly affected by Mg^{2+} (lanes 1–3). The observed effects of Mg^{2+} were not caused by an unspecific influence of ionic strength since they could not be mimicked by addition of NaCl (lane 4).

We have also tested the effect of ATP in absence of Ca^{2+} and Mg^{2+} (Fig. 5). Under these conditions the Ca^{2+}-ATPase is not phosphorylated, and ATP binding *per se* has the same effect as Mg^{2+} binding: disappearance of the X_2 fragment and only a slight change in the distribution of A'_1 and A''_1 fragments.

In Fig. 6 the dependence of the tryptic cleavage pattern on Ca^{2+} concentration has been examined in more detail both in nonphosphorylating and in phosphorylating conditions. Lanes 1–4 show the effect of varying Ca^{2+} between 10^{-9} and 10^{-7} M in absence of ATP. A Ca^{2+}-induced decrease in A'_1/A''_1 concentration ratio (from 0.6 to 0.15) occurs rather abruptly between $10^{-8.5}$ and 10^{-8} M Ca^{2+} corresponding to high affinity binding of Ca^{2+} to transport sites. Lanes 5–7 show that the Ca^{2+} effect is shifted to a millimolar concentration range in the presence of ATP and Mg^{2+} (i.e., under phosphorylating conditions). Removal of Mg^{2+} in presence of 2 mM Ca^{2+} changes the distribution of A'_1 and A''_1 peptides in favor of the Ca^{2+} pattern (lane 8). Lane 9 shows that in contrast to ATP the nonphosphorylating ATP analogue AdoPP[NH]P has little effect on the Ca^{2+} concentration required for change in cleavage pattern. Since the unphosphorylated reaction intermediates in the Ca^{2+}-ATPase cycle (Scheme 1) do not accumulate in significant amounts in the steady-state situation achieved in presence of millimolar ATP, it may be assumed that the two different cleavage patterns observed in this condition

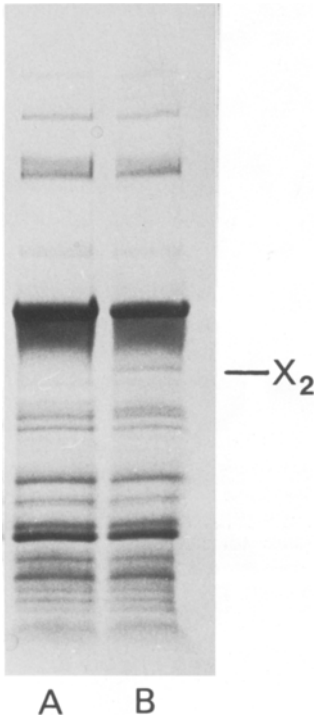

Fig. 5. Effect of ATP binding on tryptic cleavage of Ca^{2+}-ATPase. Digestion of purified Ca^{2+}-ATPase membranes with trypsin (5 μg/100 μg Ca^{2+}-ATPase) was performed for 2 min at 20°C as described in Materials and Methods in presence of 30 mM NaCl, 50 mM Tes/Tris (pH 8.0) and 1 mM EGTA with (*A*) or without (*B*) 1 mM ATP

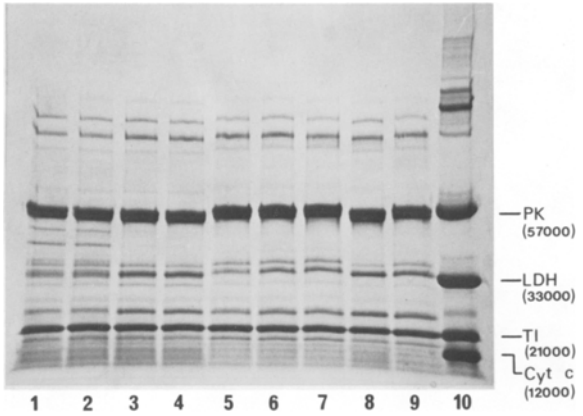

Fig. 6. Effect of Ca^{2+} concentration and phosphorylation on tryptic cleavage of Ca^{2+}-ATPase. Digestion of purified Ca^{2+}-ATPase membranes with trypsin (5 μg/100 μg Ca^{2+}-ATPase) was performed for 5 min at 20°C in 30 mM NaCl, 50 mM Tes/Tris (pH 8.0) as described in Materials and Methods. Further additions present during trypsinolysis are indicated below. Lane 1: 1 mM EGTA (pCa > 9.0). Lane 2: 78 μM $CaCl_2$, 0.2 mM EGTA (pCa = 8.5). Lane 3: 134 μM $CaCl_2$, 0.2 mM EGTA (pCa = 8.0). Lane 4: 180 μM $CaCl_2$, 0.2 mM EGTA (pCa = 7.3). Lane 5: 50 μM $CaCl_2$, 10 mM $MgCl_2$, 2 mM ATP. Lane 6: 500 μM $CaCl_2$, 10 mM $MgCl_2$, 2 mM ATP. Lane 7: 2.0 mM $CaCl_2$, 10 mM $MgCl_2$, 2 mM ATP. Lane 8: 2.0 mM $CaCl_2$, 2 mM ATP. Lane 9: 50 μM $CaCl_2$, 10 mM $MgCl_2$, 2 mM AdoPP[NH]P. Under the conditions of highest ATP hydrolysis rate (lane 5) the ATP hydrolyzed during the experiment amounted to less than 30% of the ATP initially present

represent ADP-sensitive and ADP-insensitive phosphoenzymes, respectively. The effects of Ca^{2+} and Mg^{2+} are in accordance with this interpretation. Ca^{2+} binding to low affinity translocation sites on the ADP-insensitive phosphoenzyme shifts the equilibrium in favor of ADP-sensitive phosphoenzyme [10]. A similar change is induced by decreasing the Mg^{2+} concentration, presumably by an effect of substitution of Ca^{2+} at the phosphorylation site for Mg^{2+} [3]. Therefore the data in Fig. 6 indicate that the two phosphorylated states of the Ca^{2+}-pump protein have tryptic cleavage patterns similar to the corresponding unphosphorylated states, E_1 and E_2, in accordance with the notation in Scheme 1 (ADP-sensitive phosphoenzyme = E_1P, ADP-insensitive phosphoenzyme = E_2P).

Electrophoresis at low pH of phosphorylated peptides provides a way of identifying cleaved fragments that accept ^{32}P from [$\gamma^{32}P$]-ATP. As can be seen in Fig. 7, ^{32}P labeled A fragment is well separated from the ^{32}P-labeled A_1 peptides. The distribution of radioactivity associated with the various peaks of Fig. 7 is in agreement with an increased rate of secondary cleavage of A in the presence of Ca^{2+}. Separate A_1' and A_1'' peaks are not seen with the acid gel system. When the amounts of radioactivity associated with the A_1 peaks of Fig. 7*B* and *C* are related quantitatively to the relative concentrations of A_1' and A_1'' estimated by gel scanning (Fig. 2), it is evident that the data are consistent only if A_1'' is assumed to be phosphorylated. The fragment (X_2) migrating between B and A_1' (Fig. 2*B*) can also be identified on stained acid gels, but this peptide does not contribute radioactivity. Therefore it is likely to be derived from the B fragment of the Ca^{2+}-ATPase polypeptide.

This technique for separation of phosphopeptides allows direct comparison of the properties of intact Ca^{2+}-ATPase with those of the phosphorylated fragments arising from tryptic cleavage. In Fig. 8, the effect of tryptic cleavage on the distribution of ADP-sensitive and ADP-insensitive phosphoenzyme species has been examined by electrophoresis at low pH after phosphorylation of the digested Ca^{2+}-ATPase with [$\gamma^{32}P$]-ATP and dephosphorylation for 5 sec in presence of ADP. It is seen that the relative amount of ADP-insensitive phosphoenzyme in the A_1 fragment is reduced as compared to the A fragment (Fig. 8). Data from this and similar experiments are shown in Table 2 together

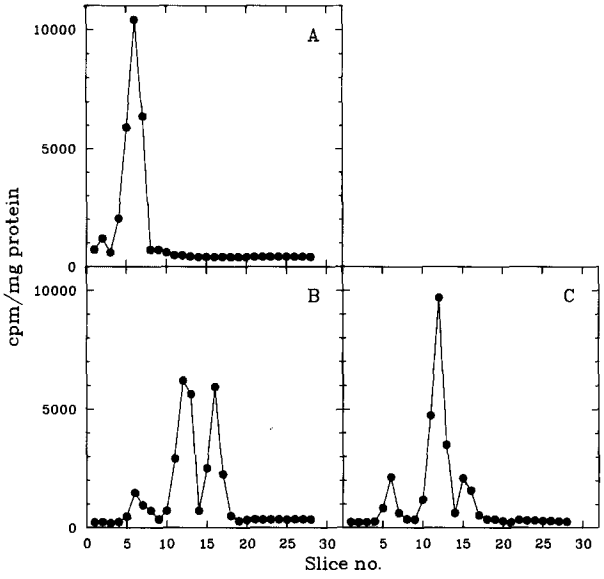

Fig. 7. Phosphorylation of tryptic fragments of Ca^{2+}-ATPase formed in presence and absence of Ca^{2+}. Purified Ca^{2+}-ATPase membranes were digested for 5 min with trypsin under conditions similar to those of Fig. 2. After termination of the reaction with trypsin inhibitor $MgCl_2$ and $CaCl_2$ were added to obtain final concentrations of 10 mM Mg^{2+} and 200 μM free Ca^{2+}, and phosphorylation with [γ^{32}P]-ATP was performed at 0°C as described in Materials and Methods. After gel electrophoresis at pH 2.4 the gel was sliced and radioactivity measured. The ordinate and abcissa show radioactivity per slice per mg protein applied to the gel and slice numbers, respectively. *A*, control incubated in absence of trypsin; *B*, sample treated with trypsin in presence of 50 μM $CaCl_2$; *C*, sample treated with trypsin in presence of 1 mM EGTA

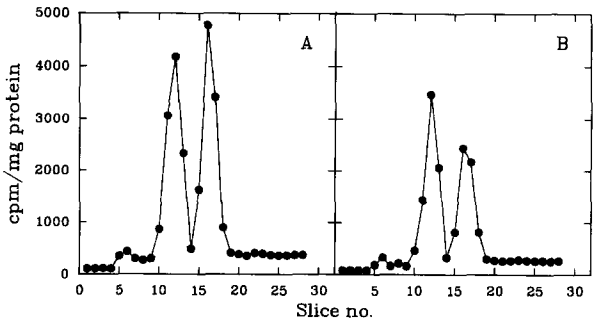

Fig. 8. ADP sensitivity of phosphorylated tryptic fragments of Ca^{2+}-ATPase. Purified Ca^{2+}-ATPase membranes were digested for 7 min with trypsin under conditions similar to those of Fig. 2*A*. After termination of the reaction with trypsin inhibitor, $MgCl_2$ and EGTA were added to produce final concentrations of 10 mM Mg^{2+} and 10^{-6} M Ca^{2+}, and phosphorylation with [γ^{32}P]-ATP was performed at 0°C as described in Materials and Methods. After 30 sec the reaction was quenched (*A*) or 1 mM ADP + 1 mM EGTA were added for 5 sec before quenching (*B*) to allow dephosphorylation of the ADP-sensitive phosphoenzyme. Following gel electrophoresis at pH 2.4, the gel was sliced and radioactivity was measured. The ordinate and abcissa show radioactivity per slice per mg protein applied to the gel and slice number, respectively

with results obtained without prior digestion. At a relatively low Ca^{2+} concentration (10^{-6} M) as much as 84% of the phosphoenzyme of the intact chain is ADP insensitive. However, only 71 and 56% of the phosphoenzymes formed from A and A_1 fragments, respectively, are ADP insensitive. At higher Ca^{2+} concentration the amount of ADP-insensitive phosphoenzyme is reduced in the intact chain in agreement with previous observations [3], and a further reduction is seen for the A_1 fragments. A similar reduction of ADP-insensitive phosphoenzyme was observed after chymotryptic cleavage (Table 2). The data thus show that tryptic cleavage of fragment A to A_1 as well as chymotryptic cleavage process a shift in conformational equilibria of the phosphoenzyme in direction of the ADP sensitive E_1P form.

The results described above indicate that the major conformational states of membrane-bound Ca^{2+}-ATPase outlined in Scheme 1 can be identified by their characteristic tryptic cleavage pattern. The next question to be addressed is whether these conformational changes occur within a protomer Ca^{2+}-ATPase unit or if association between subunits is required to elicit the transitions detected by proteolytic cleavage. We therefore examined the digestion patterns of Ca^{2+}-ATPase after solubilization in non-ionic detergent under conditions where the protein is predominantly monomeric (M_r = 115,000) as evidenced by sedimentation velocity studies and HPLC on TSK G-3000 SW columns. In absence of Ca^{2+} as well as other ligands the tryptic degradation to small peptides is very fast due to the instability of the soluble preparation in these conditions [4, 32]. However, significant stabilization can be achieved by inclusion of 10 mM Mg^{2+} in the medium (Table 3). Furthermore, when solubilization is performed after binding of vanadate the monomeric Ca^{2+}-ATPase preparation stays stable for hours (Table 3). Figure 9 shows the tryptic cleavage patterns of the soluble monomeric Ca^{2+}-ATPase in presence and absence of vanadate (*compare* lanes 1–2 with lanes 5–6). In contrast to the cleavage of vanadate-bound enzyme in the membrane (Fig. 1*D* and lanes 3–4 of Fig. 9) degradation of the soluble monomer does not cease after the primary split. However, formation of A_1'' is completely inhibited by vanadate, and the vanadate reacted E_2 state of the soluble monomeric Ca^{2+}-ATPase therefore resembles the E_2 and E_2P states of the membranous enzyme. The unusual low cleavage rate observed for membrane-bound Ca^{2+}-ATPase after vanadate binding may result from protein-protein interactions in ordered semicrystalline

Table 2. Effect of tryptic and chymotryptic cleavage on ADP sensitivity of phosphorylated Ca^{2+}-ATPase formed from [γ^{32}P]-ATP

Conditions of phosphorylation	ADP-insensitive EP		
	115 kD (%)	A (%)	A_1 (%)
Trypsin treated membrane bound Ca^{2+}-ATPase at 10^{-6} M free Ca^{2+}	84	71	56
Trypsin-treated membrane-bound Ca^{2+}-ATPase at 200 μM free Ca^{2+}	19	22	12
Trypsin-treated soluble monomeric Ca^{2+}-ATPase at 200 μM free Ca^{2+}	70	71	45
Chymotrypsin-treated membrane-bound Ca^{2+}-ATPase at 10^{-6} M free Ca^{2+}	88	Chymotryptic fragments grouped together 70%	

Tryptic cleavage and phosphorylation assay were carried out as described for Fig. 8 except that the final concentration of free Ca^{2+} during phosphorylation was varied as indicated. The amount of ADP-insensitive phosphoenzyme (E_2P) is shown as percentage of total phosphoenzyme (E_1P + E_2P) measured in the same samples. Undigested control samples were electrophoresed and otherwise processed as the digested samples. The soluble Ca^{2+}-ATPase was digested and assayed in the presence of 5 mg $C_{12}E_8$/ml. Chymotryptic digestion was carried out as described for Fig. 3, lane 1. In this case the various fragments were not well separated in the acid gel and are therefore grouped together.

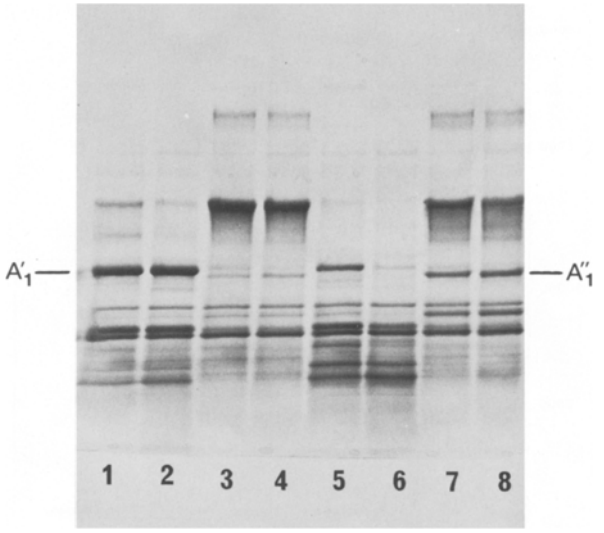

Fig. 9. Tryptic cleavage of soluble monomeric Ca^{2+}-ATPase after binding of vanadate or Ca^{2+}. Ca^{2+}-ATPase membranes (0.5 mg/ml) (which in some cases had been preincubated with vanadate) were solubilized by addition of $C_{12}E_8$ (5 mg/ml) and digested with trypsin (5 μg/100 μg Ca^{2+}-ATPase) at 20°C as described in Materials and Methods. Lane 1: 10 min digestion after preincubation for 24 hr in presence of 10 mM $MgCl_2$, 1 mM EGTA and 1 mM Na_3VO_4. Lane 2: 30 min digestion in the same conditions as for lane 1. Lane 3: Control enzyme in membranous form (no $C_{12}E_8$ added) preincubated and digested as the soluble enzyme of lane 1. Lane 4: 30 min digestion in the same conditions as for lane 3. Lane 5: Soluble Ca^{2+}-ATPase digested for 10 min in presence of 10 mM $MgCl_2$ and 1 mM EGTA. Lane 6: 30 min digestion in the same conditions as for lane 5. Lane 7: Soluble enzyme digested for 10 min in presence of 50 μM $CaCl_2$ and 10 mM $MgCl_2$. Lane 8: 30 min digestion in the same conditions as for lane 7

arrays in the plane of the membrane [15, 43]. These arrays are disrupted by detergent solubilization, although the soluble monomeric Ca^{2+}-ATPase retains the ability to bind vanadate. Figure 9, lanes 7–8, show that in the presence of Ca^{2+}, i.e. in the E_1 state, the tryptic digestion pattern of soluble monomeric Ca^{2+}-ATPase is identical to that of membranous enzyme. The characteristic feature of E_1 is again accumulation of A_1'' fragment. This difference between E_1 and E_2 was also observed after phosphorylation of the soluble monomeric Ca^{2+}-ATPase with ATP (Fig. 10). The relative concentrations of the ADP-sensitive and ADP-insensitive phosphorylated intermediates were varied by changing the Ca^{2+}/Mg^{2+} concentration ratio as described above for the membrane-bound Ca^{2+}-ATPase. Lane 1 of Fig. 10 shows the cleavage pattern after 2 min incubation of the soluble monomeric Ca^{2+}-ATPase with trypsin in the presence of 50 μM Ca^{2+} and 10 mM Mg^{2+}. Addition of 2 mM ADP (lane 2) does not change the digestion pattern. In contrast ATP induces almost complete disappearance of the A_1'' fragment (lane 3). This accords with the data of Table 2 (first column) and previous results [3] indicating that after solubilization the equilibrium between the phosphoenzymes is much in favor of E_2P. When the Ca^{2+}/Mg^{2+} concentration ratio is increased, the equilibrium is shifted towards E_1P, and the A_1'' fragment is produced in increasing amounts (lanes 4–7 of Fig. 10), as was also observed for membrane-bound Ca^{2+}-ATPase. In addition, cleavage of the A fragment changes the equilibrium between the phosphoenzymes in the soluble monomeric state (Table 2).

Control experiments testing unspecific effects of Ca^{2+}, Mg^{2+}, ATP and salt on proteolytic activity were performed with nitrated casein (Table 4). It is seen that relatively high concentrations of Ca^{2+} (1

Table 3. Stabilization of Ca^{2+}-free soluble monomeric Ca^{2+}-ATPase by Mg^{2+} and vanadate

Medium	Remaining Ca^{2+}-ATPase activity 30 min after solubilization (%)
1 mM EGTA	<1
1 mM EGTA + 1 mM $MgCl_2$	16
1 mM EGTA + 10 mM $MgCl_2$	65
1 mM EGTA + 10 mM $MgCl_2$ + 100 μM Na_3VO_4	101

Irreversible inactivation of Ca^{2+}-ATPase (0.5 mg/ml) in absence of Ca^{2+} was studied at 20°C in 50 mM Tes/Tris (pH 7.5), 0.1 M KCl and 5 mg/ml $C_{12}E_8$ together with the components indicated above. For binding of vanadate to Ca^{2+}-ATPase the vesicles were preincubated 1 hr before solubilization with $C_{12}E_8$. Thirty minutes after solubilization aliquots were transferred to tubes containing 0.1 mM excess Ca^{2+} in order to stop denaturation and promote dissociation of vanadate. Ca^{2+}-ATPase activity was measured 10 min later by a NADH-coupled assay as described in Materials and Methods. For this measurement the samples were diluted 100- to 200-fold. The activities are shown as percentage of controls incubated in presence of 0.1 mM Ca^{2+}

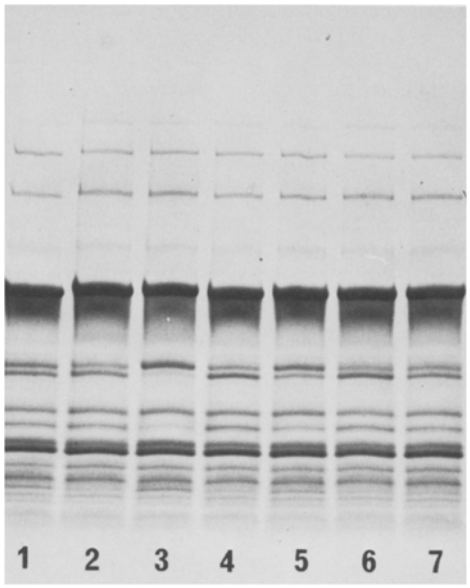

Fig. 10. Effect of phosphorylation on tryptic cleavage of soluble monomeric Ca^{2+}-ATPase. Digestion of purified Ca^{2+}-ATPase was performed for 2 min as described in Materials and Methods in the presence of 5 mg $C_{12}E_8$/ml, 30 mM NaCl, 50 mM Tes/Tris (pH 8.0) and the further additions indicated below. Lane 1: 50 μM $CaCl_2$, 10 mM $MgCl_2$. Lane 2: 50 μM $CaCl_2$, 10 mM $MgCl_2$, 2 mM ADP. Lane 3: 50 μM $CaCl_2$, 10 mM $MgCl_2$, 2 mM ATP. Lane 4: 50 μM $CaCl_2$, 2 mM $MgCl_2$. Lane 5: 50 μM $CaCl_2$, 2 mM $MgCl_2$, 2 mM ATP. Lane 6: 1 mM $CaCl_2$, 2 mM $MgCl_2$. Lane 7: 1 mM $CaCl_2$, 2 mM $MgCl_2$, 2 mM ATP

mM) increases the proteolysis rate. However, in the concentration range (10^{-8} M) required to induce changes in the digestion pattern of Ca^{2+}-ATPase no significant change in the rate of tryptic digestion of casein was seen. The concentrations of NaCl, $MgCl_2$ and ATP had only slight influence on the proteolysis rate.

Discussion

The present study has documented that the two major conformational states of Ca^{2+}-ATPase, indicated in Scheme 1, can be discriminated by their tryptic cleavage patterns. Tryptic degradation of the E_1 state results in formation of two cleavage products of the A fragment (A'_1 and A''_1). In the E_2 state trypsinolysis does not lead to formation of A''_1. In addition formation of X fragments is observed in the E_2 state in absence of Mg^{2+} and ATP, but not in the E_1 state.

In order to aid further discussion of the data we refer to the tentative model of the Ca^{2+}-ATPase polypeptide structure shown in Fig. 11. This model is based on information gathered from published sequence and labeling studies [1, 16, 27]. The primary split producing A and B fragments (split no. 1) has been shown to be located 154 amino acid residues away from the active site aspartic acid residue in the direction of the C-terminus. Split no. 2 (Fig. 11), which produces A'_1, is located in the middle of the A fragment. Split no. 3 also cleaves the A fragment and is probably located close to the N-terminus of A'_1. One split (no. 4) in the B fragment gives rise to X_2 peptide. The latter assignment is based on sequence analysis [28] and on the inability of X_2 to form acid stable phosphorylated peptide from [γ^{32}P]-ATP (present results). Our data show that the peptide bond corresponding to split no. 3 becomes more exposed to trypsin when Ca^{2+} is bound with high affinity to the unphosphorylated enzyme, i.e., in conditions favoring the E_1 state. In the phosphorylated Ca^{2+}-ATPase bond no. 3 is more exposed at Ca^{2+} concentrations in the millimolar range and at high Ca^{2+}/Mg^{2+} concentration ratios (i.e., in the ADP-sensitive phosphoenzyme) than at Ca^{2+} and Mg^{2+} concentrations favoring accumulation of ADP-insensitive phosphoenzyme (Fig. 6). Thus our findings are in accordance with the notation in Scheme 1, showing that from the point of view of tryptic cleavage pattern the two major phosphoenzyme species resemble the dephosphoforms.

Table 4. Effect of ionic conditions on tryptic digestion of nitrated Casein

Ions present in addition to 25 mM Tes/Tris	Increase in A_{428} after 5 min digestion
0.2 mM EGTA 30 mM NaCl	0.044
0.2 mM EGTA 0.18 mM $CaCl_2$ (10^{-7} M Ca^{2+}) 30 mM NaCl	0.045
50 μM $CaCl_2$ 30 mM NaCl	0.047
1 mM $CaCl_2$ 30 mM NaCl	0.051
50 μM $CaCl_2$	0.044
50 μM $CaCl_2$ 100 mM NaCl	0.043
50 μM $CaCl_2$ 30 mM NaCl 10 mM $MgCl_2$	0.050
0.2 mM EGTA 30 mM NaCl 2 mM ATP	0.044

Nitrated casein (0.5 mg/ml) was incubated for 5 min with trypsin (5 μg/ml) at 20°C in the medium indicated in the Table. After removal of undegraded casein as described in Materials and Methods absorbance was read at 428 nm

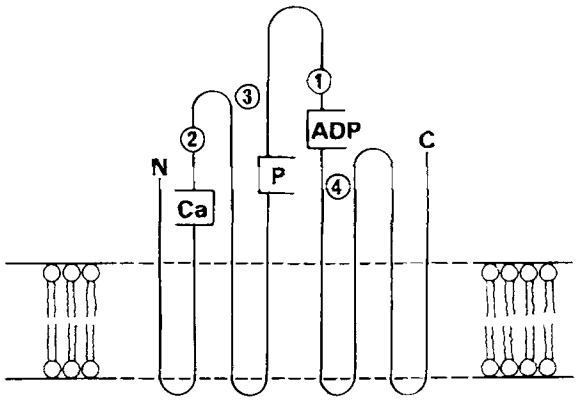

Fig. 11. Model of the structural relationship between the Ca^{2+}-ATPase polypeptide and the membrane showing the major tryptic splits studied in the present work. The precise localizations of bonds no. 3 and 4 within the respective A'_1 and B fragments are unknown. Bond no. 3 becomes more exposed to trypsin, when Ca^{2+} is bound with high affinity. Bond no. 4 is exposed in absence of Ca^{2+}, Mg^{2+} and nucleotide. *P* and *ADP* indicate the parts of the catalytic site containing the phosphorylated aspartic acid residue and the nucleotide binding region, respectively. *Ca* indicates presumptive Ca^{2+} binding sites [26, 32, 36, 39]

In conjunction with data indicating that the transition from ADP-sensitive to ADP-insensitive phosphoenzyme is accompanied by a decrease in Ca^{2+} affinity [3, 41] as well as changes in intrinsic tryptophan fluorescence [3] and in hydrophobicity of the catalytic site [14] the present evidence shows that energy transduction in the phosphoenzyme involves significant protein structural changes, which are compatible with reorientation of the Ca^{2+} sites.

The similarity of E_1 and E_1P forms deduced from the tryptic cleavage patterns and tryptophan fluorescence [3] suggests that the phosphorylation process is accompanied by structural rearrangements of rather limited size. Thus "occlusion" of Ca^{2+} in E_1P [12, 41] may result from local changes in the arrangement of carboxylic acid residues in the Ca^{2+}-transport sites, which are not reflected by changes in the tryptic degradation pattern and tryptophan fluorescence.

The changes in cleavage pattern induced by binding of Mg^{2+} and ATP in absence of Ca^{2+} (disappearance of X peptides) cannot be associated with the major conformational transitions outlined in Scheme 1, since the distribution of A'_1 and A''_1 fragments is unaltered by these ligands. It is, however, possible that the protection of bond no. 4 reflects a minor conformational change in accordance with evidence indicating an increased E_2-E_1 transition rate after binding of Mg^{2+} or ATP to E_2 [8, 17]. Alternatively, the effect of Mg^{2+} or ATP on tryptic cleavage pattern may be caused by shielding of the peptide bond by bound ligand. This is conceivable since bond no. 4 is localized close to the nucleotide binding area of the B fragment [28].

The results obtained with detergent-solubilized monomeric Ca^{2+}-ATPase in presence of Ca^{2+} and ATP (Fig. 10) show that the protein conformational states in this enzyme preparation as monitored by tryptic digestion are similar to those in the membrane-bound enzyme, thus supporting previous evidence that the functional unit in energy transduction is a single polypeptide chain with M_r 115,000 [3, 4, 29]. The observation that the presence of a phospholipid bilayer or of other Ca^{2+}-ATPase peptides in the vicinity is of so little importance for the characteristic distribution pattern of A'_1 and A''_1 fragments indicates that the change in exposure of bond no. 3 to trypsin is governed by changes in the polypeptide chain configuration or by Ca^{2+} binding *per se* and not by secondary changes in protein-lipid or protein-protein interactions. On the other hand, the disappearance of vanadate protection of bond no. 2 after solubilization in monomeric form (Fig. 9) may indicate that the slow cleavage rate of this bond observed after binding of vanadate to membranous Ca^{2+} ATPase is caused by protein-protein interac-

tions in the vanadate-induced dimeric semicrystalline state [43]. In vanadate-reacted soluble monomeric Ca^{2+}-ATPase cleavage of bond no. 3 does not occur at a measurable rate, whereas it does take place (albeit at a decreased rate) in the membranous enzyme in absence of Ca^{2+} (EGTA added) and vanadate. This indicates that vanadate "locks" the Ca^{2+}-ATPase into a very stable E_2 form, whereas the mere absence of Ca^{2+} results in a dynamic equilibrium between E_1 and E_2, in which a minor fraction of enzyme is in the E_1 state.

The cleavage data in the presence of ATP in phosphorylating conditions show that the part of the peptide chain which moves during the energy transduction process involves mainly the region close to split no. 3. Our phosphorylation data indicate that the secondary cleavages of the A fragment partially inhibit the transfer of phosphoenzyme-free energy (Fig. 8 and Table 2). It has also been shown that secondary cleavage of A interferes with high affinity binding of Ca^{2+} to the translocation sites, which probably are located in the C-terminal part of the A_2 fragment in the primary structure [26, 36, 39]. Therefore, we suggest that the region of the peptide chain in which split no. 3 is located mediates the contact between the Ca^{2+} sites and the phosphorylation site in the tertiary structure, allowing a concerted movement of the Ca^{2+} sites and part of the catalytic site during the energy transfer process. Since the phosphorylated aspartic acid residue is likely to be in a more hydrophobic environment in E_2P than in E_1P [10, 14] it is conceivable that segments of the A fragment containing the phosphorylation site and the Ca^{2+} sites move deeper into the protein structure during the E_1P to E_2P transition. The same conformational change could reasonably well lead to an increased exposure of bond no. 4 to trypsin in absence of protecting ATP or Mg^{2+}.

We thank Liselotte Madsen and Lene Jacobsen for excellent technical assistance. This investigation has been supported by the Danish Medical Research Council and the Carlsberg Foundation.

References

1. Allen, G., Trinnaman, B.J., Green, N.M. 1980. The primary structure of the calcium ion-transporting adenosine triphosphatase protein of rabbit skeletal sarcoplasmic reticulum. *Biochem. J.* **187:**591–616
2. Andersen, J.P., Fellmann, P., Møller, J.V., Devaux, P.F. 1981. Immobilization of a spin-labeled fatty acid chain covalently attached to Ca^{2+}-ATPase from sarcoplasmic reticulum suggests an oligomeric structure. *Biochemistry* **20:**4928–4936
3. Andersen, J.P., Lassen, K., Møller, J.V. 1985. Changes in Ca^{2+} affinity related to conformational transitions in the phosphorylated state of soluble monomeric Ca^{2+}-ATPase from sarcoplasmic reticulum. *J. Biol. Chem.* **260:**371–380
4. Andersen, J.P., Møller, J.V., Jørgensen, P.L. 1982. The functional unit of sarcoplasmic reticulum Ca^{2+}-ATPase: Active site titration and fluorescence measurements. *J. Biol. Chem.* **257:**8300–8307
5. Andersen, J.P., Skriver, E., Mahrous, T.S., Møller, J.V. 1983. Reconstitution of sarcoplasmic reticulum Ca^{2+}-ATPase with excess lipid: Dispersion of the pump units. *Biochim. Biophys. Acta* **728:**1–10
6. Avruch, J., Fairbanks, G. 1972. Demonstration of a phosphopeptide intermediate in the Mg^{2+}-dependent, Na^+- and K^+-stimulated adenosine triphosphatase reaction of the erythrocyte membrane. *Proc. Natl. Acad. Sci. USA* **69:**1216–1220
7. Champeil, P., Bastide, F., Taupin, C., Gary-Bobo, C.M. 1976. Spin labelled sarcoplasmic reticulum vesicles: Ca^{2+}-induced spectral changes. *FEBS Lett.* **63:**270–272
8. Champeil, P., Gingold, M.P., Guillain, F., Inesi, G. 1983. Effect of magnesium on the calcium-dependent transient kinetics of sarcoplasmic reticulum ATPase studied by stopped flow fluorescence and phosphorylation. *J. Biol. Chem.* **258:**4453–4458
9. Coan, C., Verjovski-Almeida, S., Inesi, G. 1979. Ca^{2+} regulation of conformational states in the transport cycle of spin-labelled sarcoplasmic reticulum ATPase. *J. Biol. Chem.* **254:**2968–2974
10. De Meis, L. 1981. The Sarcoplasmic Reticulum. John Wiley & Sons, New York
11. Dupont, Y. 1976. Fluorescence studies of the sarcoplasmic reticulum calcium pump. *Biochem. Biophys. Res. Commun.* **71:**544–550
12. Dupont, Y. 1980. Occlusion of divalent cations in the phosphorylated calcium pump of sarcoplasmic reticulum. *Eur. J. Biochem.* **109:**231–238
13. Dupont, Y., Bennett, N., Lacapere, J. 1982. ATP-induced conformational transitions of the Ca^{2+}-ATPase of sarcoplasmic reticulum. *Ann. N.Y. Acad. Sci.* **402:**569–572
14. Dupont, Y., Pougeois, R. 1983. Evaluation of H_2O activity in the free or phosphorylated catalytic site of Ca^{2+}-ATPase. *FEBS Lett.* **156:**93–98
15. Dux, L., Martonosi, A. 1983. Ca^{2+}-ATPase crystals in sarcoplasmic reticulum: The effect of trypsin digestion. *J. Biol. Chem.* **258:**10111–10115
16. Green, N.M., Allen, G., Hebdon, G.M. 1980. Structural relationship between the calcium- and magnesium-transporting ATPase of sarcoplasmic reticulum and the membrane. *Ann. N.Y. Acad. Sci.* **358:**149–158
17. Guillain, F., Champeil, P., Lacapere, J., Gingold, M.P. 1981. Stopped flow and rapid quenching measurement of the transient steps induced by calcium binding to sarcoplasmic reticulum adenosine triphosphatase. *J. Biol. Chem.* **256:**6140–6147
18. Guillain, F., Gingold, M.P., Büschlen, S., Champeil, P. 1980. A direct fluorescence study of the transient steps induced by calcium binding to sarcoplasmic reticulum ATPase. *J. Biol. Chem.* **255:**2072–2076
19. Hymel, L., Maurer, A., Berenski, C., Jung, C.Y., Fleischer, S. 1984. Target size of calcium pump protein from skeletal muscle sarcoplasmic reticulum. *J. Biol. Chem.* **259:**4890–4895
20. Ikemoto, N., Sreter, F.A., Gergely, J. 1971. Structural features of the vesicles of FSR: Lack of functional role in Ca^{2+}-

uptake and ATPase activity. *Arch. Biochem. Biophys.* **147:**571–582
21. Imamura, Y., Saito, K., Kawakita, M. 1984. Conformational change of Ca^{2+}, Mg^{2+}-adenosine triphosphatase of sarcoplasmic reticulum upon binding of Ca^{2+} and adenyl-5'-yl-imidodiphosphate as detected by trypsin sensitivity analysis. *J. Biochem.* **95:**1305–1313
22. Inesi, G., Scales, D. 1974. Tryptic cleavage of sarcoplasmic reticulum protein. *Biochemistry* **13:**3298–3306
23. Jørgensen, P.L. 1983. Mechanism of the Na^+,K^+ Pump. Protein structure and conformations of the pure (Na^+ + K^+)-ATPase. *Biochim. Biophys. Acta* **694:**27–68
24. Jørgensen, P.L., Petersen, J. 1975. Purification and characterization of (Na^+,K^+)-ATPase: V. Conformational changes in the enzyme. Transitions between the Na-form and the K-form studied with tryptic digestion as a tool. *Biochim. Biophys. Acta* **401:**399–415
25. Laemmli, U.K. 1970. Cleavage of structural proteins during the assembly of the head of bacteriophage T4. *Nature (London)* **227:**680–685
26. Lüdi, J., Hasselbach, W. 1984. Separation of the tryptic fragments of sarcoplasmic reticulum ATPase with high performance liquid chromatography. Identification of the calcium binding site. *FEBS Lett.* **167:**33–36
27. MacLennan, D.H., Reithmeier, A.F. 1982. The structure of the Ca^{2+}/Mg^{2+}-ATPase of sarcoplasmic reticulum. *In:* Membranes and Transport. A.N. Martonosi, editor. pp. 567–571. Plenum, New York
28. Marcsek, Z., Nelson, R., Ikemoto, N. 1983. Bivalent cation dependent conformational changes of the sarcoplasmic reticulum Ca^{2+}-ATPase modify the second tryptic cleavage site. Abstracts of the 15th FEBS Meeting, Brussels 1983
29. Martin, D.W., Tanford, C., Reynolds, J.A. 1984. Monomeric solubilized sarcoplasmic reticulum Ca pump protein: Demonstration of Ca binding and dissociation coupled to ATP hydrolysis. *Proc. Natl. Acad. Sci. USA* **81:**6623–6626
30. Martonosi, A.N., Beeler, T.J. 1983. Mechanism of Ca^{2+}-transport by sarcoplasmic reticulum. *In:* Handbook of Physiology. Section 10: Skeletal Muscle. pp. 417–485. American Physiological Society, Bethesda
31. Migala, A., Agostini, B., Hasselbach, W. 1973. Tryptic fragmentation of the calcium transport system in the sarcoplasmic reticulum. *Z. Naturforsch.* **28c:**178–182
32. Møller, J.V., Andersen, J.P., Maire, M. le 1982. The sarcoplasmic reticulum Ca^{2+}-ATPase. *Mol. Cell. Biochem.* **42:**83–107
33. Møller, J.V., Lind, K.E., Andersen, J.P. 1980. Enzyme kinetics and substrate stabilization of detergent-solubilized and membraneous (Ca^{2+} + Mg^{2+})-activated ATPase from sarcoplasmic reticulum. *J. Biol. Chem.* **255:**1912–1920
34. Murphy, A.J. 1976. Sulfhydryl group modification of sarcoplasmic reticulum membranes. *Biochemistry* **15:**4492–4496
35. Pick, U., Karlish, S.J.D. 1982. Regulation of the conformational transition in the Ca-ATPase from sarcoplasmic reticulum by pH, temperature and calcium ions. *J. Biol. Chem.* **257:**6120–6126
36. Pick, U., Racker, E. 1979. Inhibition of the Ca^2-ATPase from sarcoplasmic reticulum by dicyclohexylcarbodiimide: Evidence for location of the Ca^2-binding site in a hydrophobic region. *Biochemistry* **18:**108–113
37. Pickart, C.M., Jencks, W.P. 1984. Energetics of the calcium-transporting ATPase. *J. Biol. Chem.* **259:**1629–1643
38. Poduslo, J.F., Rodbard, D. 1980. Molecular weight estimation using sodium dodecyl sulfate-pore gradient electrophoresis. *Anal. Biochem.* **101:**394–406
39. Scott, T.L., Shamoo, A.E. 1984. Distinction of the roles of the two high-affinity calcium sites in the functional activities of the Ca^{2+}-ATPase of sarcoplasmic reticulum. *Eur. J. Biochem.* **143:**427–436
40. Stewart, P.S., MacLennan, D.H. 1974. Surface particles of sarcoplasmic reticulum membranes: Structural features of the adenosine triphosphatase. *J. Biol. Chem.* **249:**985–993
41. Takisawa, H., Makinose, M. 1983. Occlusion of calcium in the ADP-sensitive phosphoenzyme of the adenosine triphosphatase of sarcoplasmic reticulum. *J. Biol. Chem.* **258:**2986–2992
42. Tanford, C. 1984. Twenty questions concerning the reaction cycle of the sarcoplasmic reticulum calcium pump. *CRC Crit. Rev. Biochem.* **17:**123–151
43. Taylor, K., Dux, L., Martonosi, A. 1984. Structure of the vanadate-induced crystals of sarcoplasmic reticulum Ca^{2+}-ATPase. *J. Mol. Biol.* **174:**193–204
44. Thorley-Lawson, D.A., Green, N.M. 1973. Studies on the location and orientation of proteins in the sarcoplasmic reticulum. *Eur. J. Biochem.* **40:**403–413
45. Vianna, A.L. 1975. Interaction of calcium and magnesium in activating and inhibiting the nucleoside triphosphatase of sarcoplasmic reticulum vesicles. *Biochim. Biophys. Acta* **410:**389–406
46. Yamada, S., Ikemoto, N. 1978. Distinction of thiols involved in the specific reaction steps of the Ca^{2+}-ATPase of the sarcoplasmic reticulum. *J. Biol. Chem.* **253:**6801–6807

Received 30 May 1985